Original Article

www.anatomy.org.tr
*Received: June 11, 2020; Accepted: July 27, 2020*
doi:10.2399/ana.20.779018

anatomy
An International Journal of Experimental and Clinical Anatomy

# Three-dimensional architecture of the great toe muscles: functional implications in hallux valgus

**Valera Castanov[1], Maxine D. Vienneau[1], Takamitsu Arakawa[2], S. Ahmed Hassan[1], Anne Agur[1], Diane Tyczynski[3]**

[1]*Division of Anatomy, Department of Surgery, University of Toronto, Toronto, Ontario, Canada*
[2]*Department of Rehabilitation Sciences, Kobe University Graduate School of Health Sciences, Sumaku, Kobe, Japan*
[3]*Chiropody Program, The Michener Institute of Education, University Health Network, Toronto, Canada*

## Abstract

**Objectives:** Imbalance of great toe musculature has been identified as a factor in the development of hallux valgus. The musculoaponeurotic architecture, an important determinant of function, has not been investigated volumetrically in the great toe musculature. The purpose of this study was to reconstruct the abductor halluces (ABDH), adductor halluces (ADH), flexor hallucis brevis medial (FHBM) and lateral (FHBL) heads volumetrically and to quantify and compare their architectural parameters and functional characteristics.

**Methods:** Ten formalin-embalmed specimens were dissected, digitized and modelled (Autodesk Maya®). Fiber bundle length (FBL) and physiological cross-sectional area (PCSA) of the muscles were compared using descriptive and parametric statistics.

**Results:** The spatial arrangement of aponeuroses (AP) / fiber bundles (FB) and architectural parameters varied throughout the volume of each muscle. The PCSA of the medial (ABDH/FHBM) and lateral (ADH/FHBL) musculature was similar; however, the medial musculature had significantly greater mean FBL.

**Conclusion:** Each muscle had varying AP/FB arrangement. The similar PCSA of the medial and lateral musculature suggests that their relative force generating capabilities are balanced in asymptomatic individuals.

**Keywords:** fiber bundle length; great toe; hallux valgus; muscle architecture; PCSA; pennation angle; volume

Anatomy 2020;14(2):77–85 

## Introduction

Hallux valgus (HV) is a common condition of the great toe (hallux) characterized by lateral deviation of the hallux and medial shift of the first metatarsal with an estimated prevalence of 23% in individuals aged 18–65 and 35% in those over age 65.[1] The pathogenesis of HV is multifactorial with numerous etiological factors, one being the imbalance of the lateral and medial muscles of the great toe.[2-4] EMG studies investigating the activation of the great toe musculature in subjects with HV are scarce. Incel et al.[5] reported decreased activation of abductor hallucis relative to adductor hallucis in subjects with HV, whereas Iida and Basmajian[6] found decreased adductor hallucis activity during attempted adduction and no abductor hallucis activity during attempted abduction. In addition, Mortka et al.[7] and Hoffmeyer et al.[3] reported that the activation of abductor hallucis in patients with HV was reduced when compared to normal controls.

In order to investigate the role of muscle imbalance in HV, normal muscle architecture must be understood, as it is the primary determinant of function.[8] Muscle architecture is the arrangement of the contractile (fiber bundles) and connective tissue (aponeuroses/tendons) elements within the muscle volume. The location and spatial orientation of these elements play an important role in force transmission from the fiber bundles (FBs) to the muscle

*This study was a part of first author's (Valera Castonov) PhD thesis entitled "Three-dimensional musculoaponeurotic architecture of the human lower limb and its functional implications", Institute of Medical Science, University of Toronto, 2019.*

attachment site(s).[9,10] In addition to their spatial arrangement, FBs and aponeuroses/tendons can be characterized by quantifiable architectural parameters that are indicative of their relative functional capabilities. Architectural parameters include fiber bundle length (FBL), a measure of relative excursion capability; pennation angle (PA), a factor influencing force generation; muscle volume (MV), the size of a muscle; and physiological cross-sectional area (PCSA), the relative force generating capability of the muscle.[10,11]

Five cadaveric studies were found that investigated the architectural parameters of the great toe musculature (**Table 1**). Kura et al.,[12] Silver et al.[13] and Tosovic et al.[14] sampled 3 fiber bundles in each great toe muscle, whereas Lachowitzer et al.[15] and Ledoux et al.[16] did not report the number of FBs sampled. The site of FB sampling was from the superficial surface of the muscles,[12–14] from photographs[16] or not specified.[15] No volumetric studies were found that documented architecture of the great toe musculature in 3D space. Therefore, the purpose of this study was to: (1) determine the musculoaponeurotic architecture throughout the volume of the great toe musculature; (2) determine if the muscles are partitioned based on musculoaponeurotic architecture; (3) quantify and compare FBL, PA, MV and PCSA of the medial and lateral muscles of the great toe and their partitions, if present; (4) compare the relative excursion and relative force generation capabilities of the medial and lateral musculature.

## Materials and Methods

Ten formalin embalmed cadaveric specimens (5M/5F; mean age: 77.9±11.5 years) were used in this study. Specimens with visible signs of musculoskeletal pathology or previous surgery were excluded. Ethics approval was received from the University of Toronto Health Sciences Research Ethics Board (Approval number: 27210).

The ankle and foot joints were stabilized using metal plates and screws to prevent movement during digitization. The abductor hallucis (ABDH), oblique head of adductor hallucis (ADHO), transverse head of adductor hallucis (ADHT), medial head of flexor hallucis brevis (FHBM) and lateral head of flexor hallucis brevis (FHBL) were exposed by removing superficial tissues including, skin, subcutaneous tissue, plantar aponeurosis, other intrinsic muscles, tendons of extrinsic muscles and neurovascular bundles. Three screws were drilled into bony landmarks (medial malleolus, posterior calcaneus and the medial aspect of the proximal phalanx of the 1st digit) to establish a Cartesian reference frame to capture and later reconstruct the digitized data in 3D.

**Table 1**

Summary of mean architectural parameters reported in the literature. Studies include: Kura et al.;[12] Silver et al.;[13] Tosovic et al.;[14] Lachowitzer et al.[15] and Ledoux et al.[16]

| | MV ($cm^3$) | FBL (mm) | PA (°) | PCSA ($cm^2$) |
|---|---|---|---|---|
| ABDH | 15.2±5.3[12]<br>10.6±2.9[15] | 23.0±5.5[12]<br>16.5±5.2[15]<br>25.0±10.5[13] | 16.0±1.4[15]<br>16.5±7.5[16]<br>18.7±9.1[14] | 6.7±2.1[12]<br>6.9±4.8[15]<br>2.7±0.7[13]<br>3.3±1.9[14] |
| ADH | 7.7±2.3[15] | 13.7±1.2[15] | 17.0±12.0[15] | 4.6±1.9[15] |
| ADHO | 9.1±3.1[12] | 18.6±5.3[12]<br>14.3±2.0[15]<br>17.0±5.0[13] | 20.9±13.1[15]<br>9.0±7.3[16] | 4.9±1.4[12]<br>3.1±0.9[15]<br>2.3±0.4[13] |
| ADHT | 1.1±0.6[12] | 18.7±5.2[12]<br>13.1±0.5[15]<br>17.0±4.9[13] | 13.1±12.6[15]<br>13.3±7.8[16] | 0.6±0.3[12]<br>1.0±0.7[15]<br>0.4±0.3[13] |
| FHB | 5.8±1.7[15] | 14.6±0.8[15] | 18.5±5.1[15]<br>7.8±7.7[16] | 3.4±1.0[15] |
| FHBM | 3.1±1.3[12] | 17.5±4.8[12]<br>15.5±1.5[15]<br>19.0±5.3[13] | 15.5±7.1[15] | 1.8±0.8[12]<br>0.7±0.3[13] |
| FHBL | 3.4±1.4[12] | 16.5±3.4[12]<br>13.6±1.5[15]<br>20.0±6.4[13] | 21.5±7.6[15] | 2.1±0.8[12]<br>0.9±0.3[13] |

**ABDH:** abductor hallucis; **ADH:** adductor hallucis; **ADHO:** oblique head of adductor hallucis; **ADHT:** transverse head of adductor hallucis; **FHB:** flexor hallucis brevis; **FHBL:** lateral head of flexor hallucis brevis; **FBL:** fiber bundle length; **FHBM:** medial head of flexor hallucis brevis; **MV:** muscle volume; **PA:** pennation angle; **PCSA:** physiological cross-sectional area.

Dissection and digitization were carried out using the same protocol for all muscles. First, the FBs on the superficial surface were delineated between attachment sites and then digitized at 2–3 mm intervals using a Microscribe® MX digitizer (Immersion Corporation, San Jose, CA, USA). The ICC for the intra-observer reliability for FB digitization was 0.995 (95% CI: 0.990–0.998) and 0.961 (95% CI: 0.800–0.986) for the inter-observer reliability.[9] Next, the digitized FBs were excised to expose deeper FBs. This process was repeated until the entire muscle had been digitized. The tendons, aponeuroses and attachment sites were also digitized as they were exposed during serial dissection. The digitized data were constructed into 3D models using Autodesk® Maya® (Autodesk Inc., San Rafael, CA, USA). The architectural parameters (FBL, distal PA [DPA], proximal PA [PPA], PCSA, MV) of the great toe muscles were computed from the digitized data using custom software developed in the laboratory.

The 3D models were used to determine the spatial arrangement and attachment sites of FBs and aponeuroses throughout the muscle volume. The sites of attachment of tendons (extramuscular) were also documented. Each muscle model was examined at the FB level to determine if intramuscular partitioning was present based on FB morphometry and attachment sites. If an intramuscular partition was identified, the architectural parameters were also computed for each partition.

The architectural parameters were then compared between whole muscles and between their intramuscular partitions using ANOVA with Tukey's post-hoc test, and subsequent two-tailed t-tests to determine whether architectural parameters were significantly different ($p<0.05$) (IBM® SPSS Statistics, IBM® Corp., Armonk, NY, USA). Based on the computed architectural parameters, the relative excursion and force-generating capabilities of the whole muscles, intramuscular partitions, and the medial (ABDH, FHBM) and lateral (ADHO, ADHT, FHBL) great toe musculature were compared.

## Results

The spatial arrangement of the FBs and aponeuroses of the great toe musculature was found to be complex and unique to each muscle. All muscles were pennate and further partitioned based on musculoaponeurotic architecture and attachment sites to aponeuroses, tendons and/or bones (**Figure 1**). The architectural parameters of these muscles varied (**Table 2**). The ADHT had the longest mean FBL (19.4±6.7 mm), whereas, FHBL had the shortest (14.1±4.2 mm). It was also found that ABDH had the largest mean muscle volume and PCSA, while ADHT the smallest. The PCSA of FHBM and FHBL were similar, approximately one third of that of ADHO.

The spatial arrangement of the fiber bundles/aponeuroses and architectural parameters of the partitions of each great toe muscle is discussed below. It is followed by analysis of the architectural parameters of the medial and lateral great toe muscles.

### Abductor Hallucis

In all specimens, the muscle belly was divided into two partitions, medial and lateral, based on the attachment of the FBs to a thick aponeurosis located between the partitions (**Figures 2a–d**). Both proximal and distal attachment

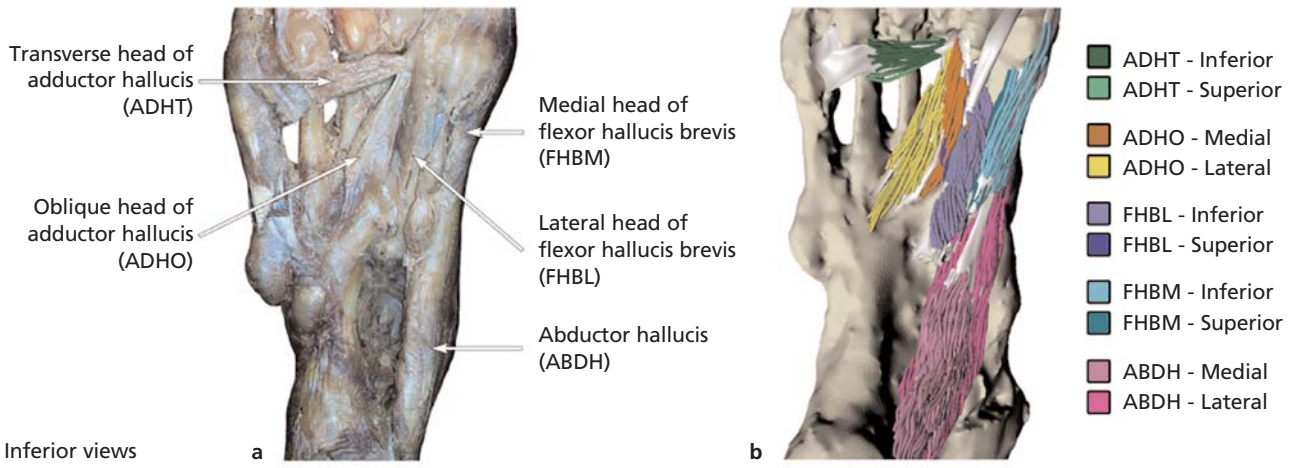


**Figure 1.** Cadaveric dissection and a three-dimensional model of the great toe musculature. (**a**) Cadaveric dissection. (**b**) Three-dimensional musculoaponeurotic model at the fiber bundle level as *in situ*.

**Table 2**
Mean architectural parameters of the intrinsic muscles of the great toe.

| Muscle | FBL (mm) | Distal PA (°) | Proximal PA (°) | PCSA (cm²) | MV (cm³) |
|---|---|---|---|---|---|
| ABDH | 17.5±6.2[a] | 16.1±9.1[e] | 16.2±9.1[i] | 4.9±1.9[m] | 8.6±3.1[o] |
| FHBM | 16.8±5.3[b] | 11.0±6.8[f] | 11.0±6.8[j] | 1.3±0.9[n] | 2.3±1.5[p] |
| FHBL | 14.1±4.2[c] | 13.0±7.6[g] | 11.2±6.4[j] | 1.8±1.2[n] | 2.6±1.7[p] |
| ADHO | 16.3±4.5[b] | 11.6±7.4[h] | 10.5±6.6[k] | 3.9±1.0[m] | 6.7±1.7[o] |
| ADHT | 19.4±6.7[d] | 13.2±7.8[g] | 13.9±8.1[l] | 0.6±0.2[n] | 1.0±0.5[p] |

Architectural parameters that are significantly different between muscles are indicated with different superscript letters; if superscript letters are the same, no statistical difference was observed (p>0.05). **ABDH:** abductor hallucis; **ADHO:** oblique head of adductor hallucis; **ADHT:** transverse head of adductor hallucis; **FBL:** fiber bundle length; **FHBL:** lateral head of flexor hallucis brevis; **FHBM:** medial head of flexor hallucis brevis; **MV:** muscle volume; **PA:** pennation angle; **PCSA:** physiological cross-sectional area.

sites of the FBs of the medial and the lateral partitions were to the medial and lateral aspects of the central aponeurosis, respectively. The aponeurosis attached posteriorly to the medial surface of the calcaneus and medial calcaneal tubercle and narrowed anteriorly to become the tendon of ABDH. The tendon of ABDH was found to attach to the medial and inferomedial surface of the medial sesamoid bone and to the medial tubercle of the base of the proximal phalanx of the great toe. The FBs of the medial and lateral partitions were arranged sequentially in overlapping layers (**Figures 2c** and **d**).

As a whole, ABDH was found to have the largest mean DPA, PPA, PCSA and MV (**Table 2**). The mean FBL, DPA and PPA of the medial partition of ABDH were significantly greater than those of the lateral partition (**Table 3**). In contrast, the PCSA and MV of the lateral partition tended to be greater, although not statistically significant.

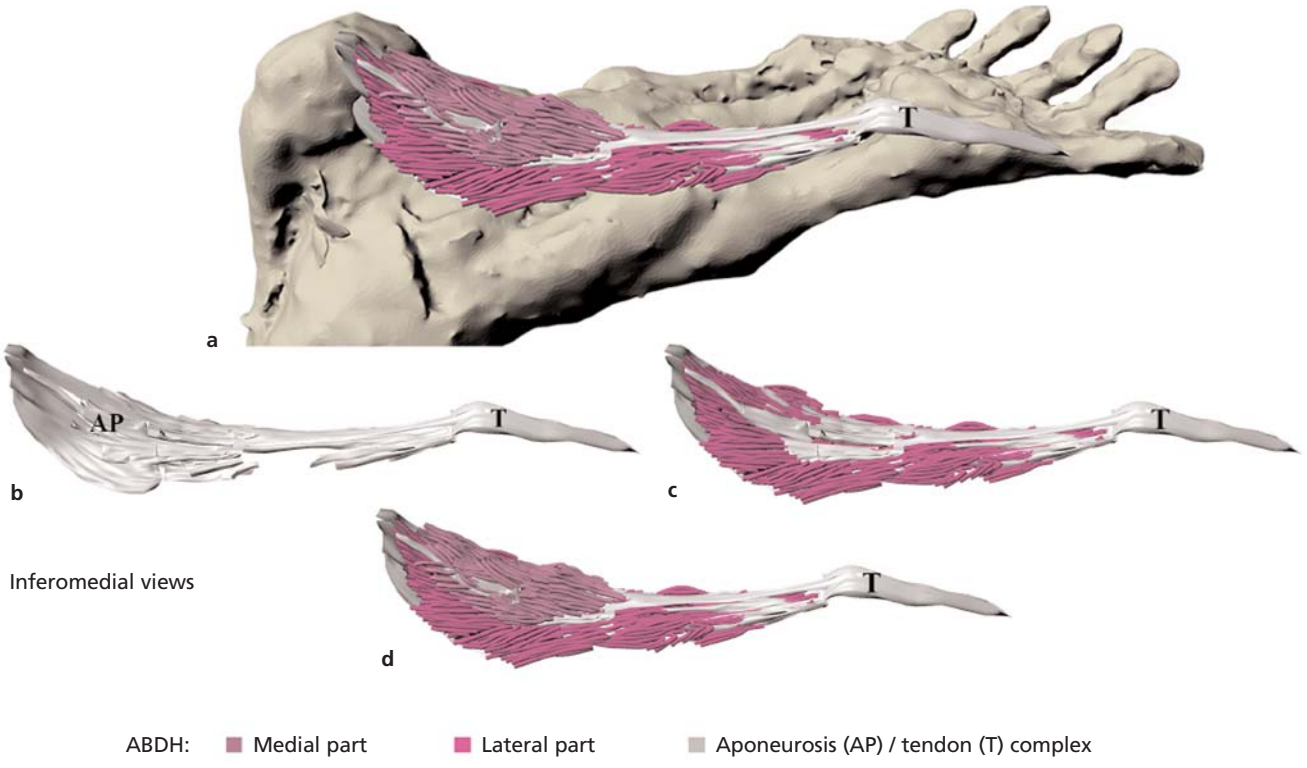


**Figure 2.** Three-dimensional musculoaponeurotic model of abductor hallucis (**ABDH**) as in situ. (**a**) Musculoskeletal model. (**b**) Aponeurosis (AP) / tendon (T) complex. (**c**) Lateral part. Fiber bundles attach to the deep (lateral) surface of the aponeurosis. (**d**) Medial and lateral parts. Fiber bundles of the medial part attach to the superficial (medial) surface of the aponeurosis.

**Table 3**

Mean architectural parameters of the partitions of the intrinsic muscles of the great toe.

| Partitions | | FBL (mm) | Distal PA (°) | Proximal PA (°) | PCSA (cm²) | MV (cm³) |
|---|---|---|---|---|---|---|
| ABDH | Medial | **18.8±7.0** | **17.4±9.9** | **16.8±9.8** | 2.0±1.2 | 3.6±2.0 |
| | Lateral | 16.6±5.4 | 15.3±8.6 | 15.9±8.6 | 2.9±1.2 | 4.9±1.9 |
| ADHO | Medial | 15.9±4.3 | 11.7±7.2 | **11.1±6.4** | **2.5±0.8** | **4.2±1.3** |
| | Lateral | **17.1±4.6** | 11.4±7.6 | 9.7±6.8 | 1.4±0.5 | 2.5±0.8 |
| ADHT | Inferior | 18.3±7.7 | **14.3±8.4** | 13.9±8.2 | 0.2±0.1 | 0.4±0.2 |
| | Superior | **19.9±6.2** | 12.7±7.5 | 13.9±8.0 | 0.3±0.1 | 0.5±0.3 |
| FHBL | Inferior | 13.9±4.3 | **13.7±7.7** | **12.2±6.5** | 0.9±0.6 | 1.2±0.7 |
| | Superior | **14.3±4.1** | 12.5±7.4 | 10.5±6.1 | 0.9±0.7 | 1.4±1.0 |
| FHBM | Inferior | **17.4±5.3** | **11.6±7.1** | 11.0±7.1 | 0.6±0.5 | 1.1±0.9 |
| | Superior | 16.3±5.3 | 10.4±6.5 | 11.1±6.5 | 0.7±0.5 | 1.2±0.8 |

Within each muscle, the bolded parameter is significantly greater than its counterpart ($p<0.05$). **ABDH:** abductor hallucis; **ADHO:** oblique head of adductor hallucis; **ADHT:** transverse head of adductor hallucis; **FBL:** fiber bundle length; **FHBL:** lateral head of flexor hallucis brevis; **FHBM:** medial head of flexor hallucis brevis; **MV:** muscle volume; **PA:** pennation angle; **PCSA:** physiological cross-sectional area.

## Adductor Hallucis

The ADHO was found to have two partitions, medial and lateral, based on their respective attachment sites to two separate aponeuroses, proximal and distal (**Figures 3a** and **b**). The FBs bridged the gap between these aponeuroses. The FBs of both partitions attached proximally to the proximal aponeurosis, and distally to the distal aponeurosis. The proximal aponeurosis attached to the base of the second, third and fourth metatarsals and adjacent tarsal bones. The distal aponeurosis merged with the medial

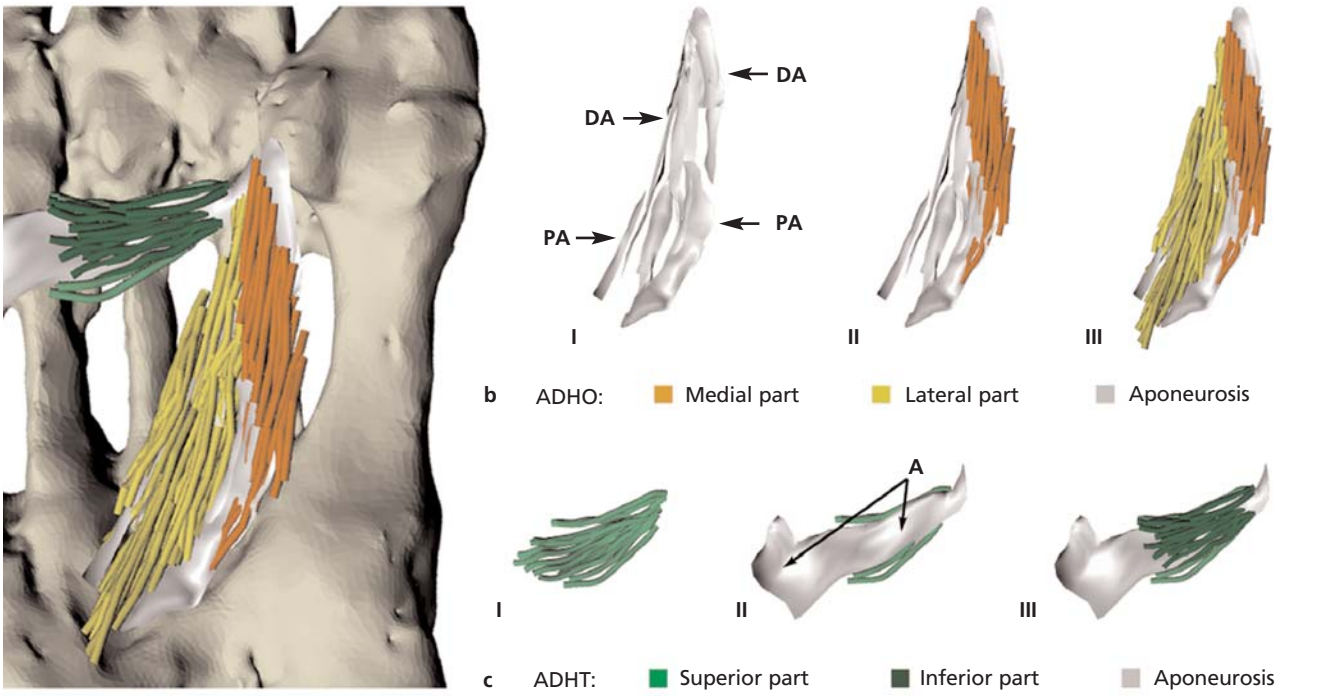


**Figure 3.** Three-dimensional musculoaponeurotic models of oblique (**ADHO**) and transverse (**ADHT**) heads of adductor hallucis as *in situ*. (**a**) Musculoskeletal model. (**b**) Serially exposed musculoaponeurotic layers of ADHO. **I-** Aponeuroses: proximal (**PA**) and distal (**DA**). **II-** Medial part. Fiber bundles are located medially and span between PA and DA. **III-** Medial and lateral parts. Fiber bundles of the lateral part are located laterally and span between PA and DA. (**c**) Serially exposed musculoaponeurotic layers of ADHT. **I-** Superior part. Fiber bundles are located on the superior surface of the aponeurosis. **II-** Aponeurosis (A). **III-** Inferior and superior parts. Fiber bundles of the inferior part are located on the inferior surface of the aponeurosis.

aponeurosis of ADHT to form a common tendon, which attached to the lateral and inferolateral surfaces of the lateral sesamoid bone and the lateral aspect of the base of the proximal phalanx.

The ADHT was also found to have two partitions; superior and inferior (**Figures 3a** and **c**). In 8 specimens, medial and lateral aponeuroses were found, and in 2 specimens, one continuous aponeurosis was present. The two partitions were delineated by FB attachment sites to superior/inferior surfaces of the lateral aponeurosis or lateral two-thirds of the continuous aponeurosis. Medially, the FBs converged onto the medial aponeurosis or to the medial third of the continuous aponeurosis. The medial aponeurotic elements became tendinous and merged with the distal aponeurosis of ADHO to form a common tendon of insertion, whereas, the lateral aponeurotic elements attached to the capsule of the third, fourth and fifth metatarsophalangeal (MTP) joints.

The mean FBL, DPA and PPA of ADHT were significantly greater than those of ADHO (**Table 2**). However, ADHO had significantly larger MV and PCSA than ADHT. The lateral partition of ADHO was found to have significantly longer mean FBL and a smaller PCSA and MV than the medial partition (**Table 3**). In ADHT, the mean FBL of the superior partition was significantly greater than that of the inferior partition.

### Flexor Hallucis Brevis

The FHBL was found to have two partitions, superior and inferior, spanning between the proximal and distal aponeuroses (**Figures 4a** and **b**). Anteriorly, the distal aponeuroses of FHBL and ADH merged into a common tendon that attached to the lateral and inferolateral surfaces of the lateral sesamoid and to the inferolateral surface of the base of the proximal phalanx. The FHBM also had two partitions, superior and inferior, bridging the proximal and distal intramuscular aponeuroses (**Figure 4c**). Distally, the inferior partition of FHBM had either a tendinous or a muscular attachment to the medial and inferomedial surfaces of the medial sesamoid bone and inferomedial surface of the base of the proximal phalanx. The aponeuroses of FHBM and FHBL attached proximally to the medial, middle and lateral cuneiforms and the long plantar ligament, lying superficial to the tendon of fibularis (peroneus) longus.

The mean FBL of FHBM was significantly greater than that of FHBL, whereas, the mean DPA of FHBM was significantly smaller (**Table 2**). The mean PPA, PCSA, and MV were similar. The mean FBL of the superior partition of FHBL was significantly longer compared to that of the inferior partition (**Table 3**). In contrast, the inferior partition of FBLM had significantly longer mean FBL than the superior partition. Furthermore, the PCSA and MV of the inferior partitions of FHBM and FHBL were smaller than those of the superior partitions.

### Medial and Lateral Great Toe Musculature

When grouped into medial (ABDH, FHBM) and lateral (ADHO, ADHT, FHBL) great toe musculature, the mean FBL, PPA and DPA of the medial muscle group were sig-

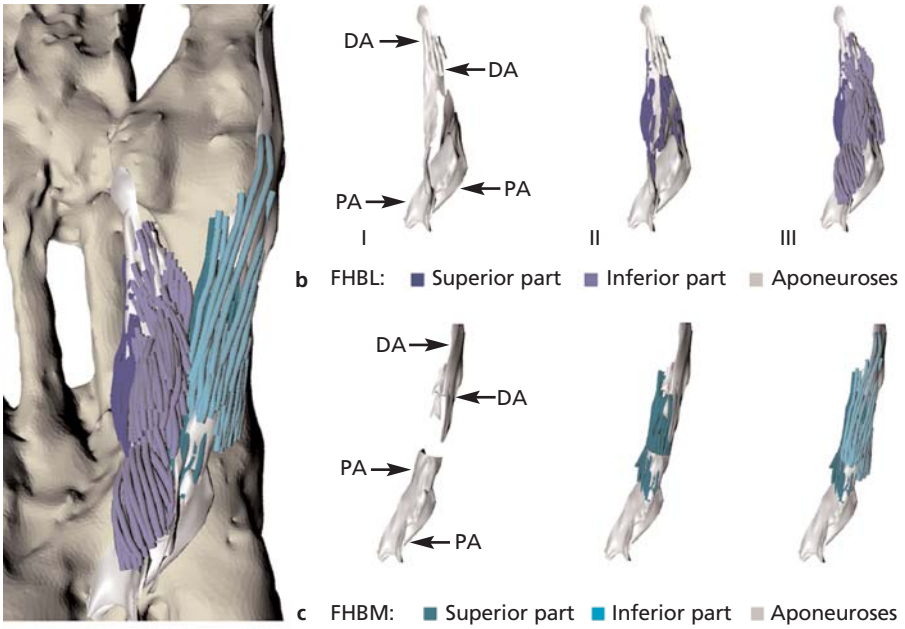


**Figure 4.** Three-dimensional musculoaponeurotic models of the lateral (**FHBL**) and medial (**FHBM**) heads of flexor hallucis brevis as *in situ*. (**a**) Musculoskeletal model. (**b**) Serially exposed musculoaponeurotic layers of FHBL. **I-** Aponeuroses: proximal (**PA**) and distal (**DA**). **II-** Superior part. Fiber bundles are located superiorly and span between PA and DA. **III-** Inferior part. Fiber bundles are located inferiorly and span between PA and DA. (**c**) Serially exposed musculoaponeurotic layers of FHBM. **I-** Aponeuroses: proximal (**PA**) and distal (**DA**). **II-** Superior part. Fiber bundles are located superiorly and span between PA and DA. **III-** Inferior part. Fiber bundles are located inferiorly and span between PA and DA.

nificantly greater (Table 4). However, the medial and lateral great toe muscles had similar PCSA (Figure 5). The largest contributor to medial musculature PCSA was ABDH (PCSA 4.9±1.9 $cm^2$), whereas, the largest contributor to lateral musculature was ADHO (PCSA 3.9±1.0 $cm^2$).

## Discussion

Our study captured and quantified the volumetric musculoaponeurotic architecture of the great toe musculature at the FB/aponeurosis level. Digitization enabled volumetric sampling of a large number of FBs, up to 580 FB per muscle. Detailed analysis of the 3D models and quantified architectural parameters demonstrated morphological and architectural differences between whole muscles and their intramuscular partitions.

The balance of the medial and lateral great toe musculature has been discussed as a possible factor in the development of hallux valgus.[3,17] In the current study, the medial (ABDH, FHBM) and lateral (ADHO, ADHT, FHBL) great toe musculature were found to have a similar PCSA, suggesting that in asymptomatic individuals the medial and lateral musculature are balanced in terms of relative force generating capabilities. This suggests that the musculature of the great toe is a factor in keeping the normal alignment of the first metatarsal, which has been shown to have the "capacity to move as an independent foot segment."[18]

The novel finding that the medial great toe musculature has significantly greater mean FBL than the lateral musculature has not been previously reported (Table 4). Since the mean FBL is an indicator of relative excursion capability, our findings suggest the medial great toe musculature has greater relative excursion capabilities than the lateral musculature. It should also be noted that the FHBM was found to have significantly longer mean FBL than FHBL and ABDH had the longest external tendon of all muscles, providing further excursion advantage to the medial musculature. In the previous literature, a small number of studies have proposed unique functional roles of ABDH that can be related to the excursion capabilities of the muscle. Wong[19] suggested that the ABDH acts as "dynamic elevator for the arch" and Headlee et al.[20] linked ABDH fatigue with navicular drop. Also, it has been reported that ABDH plays a role to "aid push-off against the ground when walking or running bipedally."[21] In a study of ABDH, flexor digitorum brevis and quadratus plantae, Kelly et al.[22] concluded that these muscles play a role in arch deformation in response to external loads.

Intramuscular partitioning of the great toe musculature has not been studied at the fiber bundle level. Previous studies are primarily descriptive; however, Kelikian,[23] Martin[24] and Tosovic et al.[14] reported partitioning in some of the great toe muscles based on the distal attachment sites. Tosovic et al.[14] found ABDH to consist of three segments, whereas Kelikian[23] found inferolateral and superomedial fiber bundles. For FHB, Martin[24] reported partitioning into superficial and deep parts. The ADHO has been characterized as having three subdivisions, medial, lateral and central, by Kelikian[23] and two parts, medial and lateral, by Martin.[24] This is in contrast to the findings of current study where each muscle was found to have 2 partitions. The 3D data collected volumetrically enabled detailed architectural analysis that has

**Table 4**

Mean architectural parameters of the medial and lateral great toe musculature.

| Muscle group | FBL (mm) | Distal PA (°) | Proximal PA (°) | PCSA ($cm^2$) |
|---|---|---|---|---|
| Medial | 17.2±5.9[a] | 14.4±8.8[c] | 14.5±8.7[e] | 6.2±0.7[g] |
| Lateral | 15.9±4.9[b] | 12.1±7.5[d] | 11.0±6.7[f] | 6.2±0.8[g] |

Architectural parameters that are significantly different between muscles are indicated with different superscript letters; if superscript letters are the same, no statistical difference was observed (p>0.05). **FBL:** fiber bundle length; **PA:** pennation angle; **PCSA:** physiological cross-sectional area.

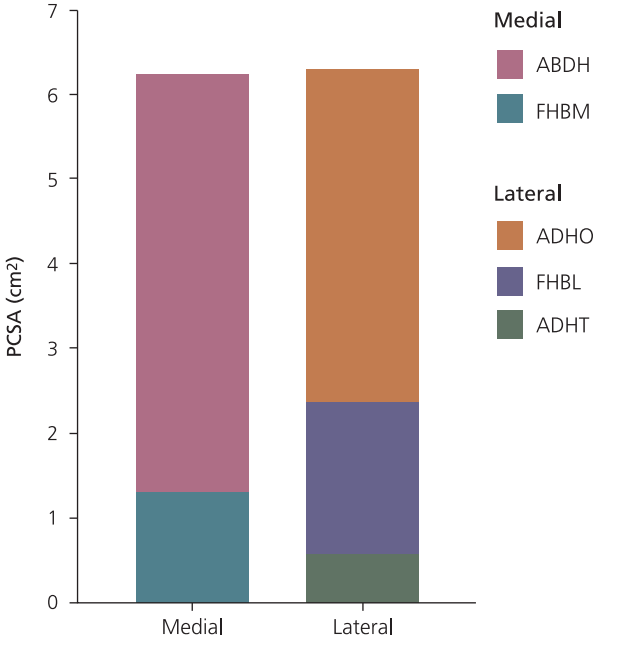


**Figure 5.** Comparison of physiological cross-sectional areas of medial and lateral great toe muscles. Medial muscles include: abductor hallucis (**ABDH**), and medial head of flexor hallucis brevis (**FHBM**). Lateral muscles include: oblique head of adductor hallucis (**ADHO**), transverse head of adductor hallucis (**ADHT**), and lateral head of flexor hallucis brevis (**FHBL**).

not been previously possible, which likely accounts for the observed differences. No studies were found that included FB attachment to intramuscular aponeuroses in their partitioning criteria, even though force transmission through aponeuroses is influenced by the arrangement and extent of FBs attaching to them. When considering architectural parameters reported in the current study, the mean FBL of the partitions within each great toe muscle were significantly different; however, the PCSA was only significantly different for the partitions of ADHO. Functionally, a factor impacting the activation of the individual partitions could be the amount of force and excursion required for dynamic movement or stabilization of the great toe. Further EMG studies are needed to determine activation patterns of the intramuscular partitions.

Imbalance of the great toe musculature has been suggested to be a causative factor in the cascade of events leading to the development of HV.[4,5] In an EMG study, Hoffmeyer et al.[3] found that ABDH activity in subjects with HV was half that of the control group with no deformity. More recently, Tas and Cetin,[25] in an *in-vivo* ultrasound study, reported that individuals with HV had smaller cross-sectional areas of ABDH and FHB than controls. In the current study, it was found that the relative force generating capabilities (PCSA) of the medial and lateral great toe musculature were balanced in the non-pathologic foot. As HV progresses, the balance of the relative force generating capabilities between the medial and lateral great toe musculature would be altered due to alterations in the biomechanical alignment of the first metatarsal and sesamoid bones.[2,4] Furthermore, the excursion and stabilization capabilities of the great toe musculature would also be changed by these alignment changes, affecting gait and arch integrity.[19,20]

A limitation of this study includes the small sample size; however, the time-consuming methodology limits the number of specimens that can be digitized and modelled. The 3D data provides the basis for further anatomical and imaging studies.

## Conclusion

This study documented the volumetric musculoaponeurotic architecture of the great toe musculature. The 3D data collection enabled analysis of the relationships of the fiber bundles, aponeuroses and their attachment sites throughout the volume of each muscle. The relative force generating capabilities (PCSA) of the medial and lateral muscles were found to be balanced in the non-pathological foot. The medial great toe muscles had a longer mean FBL, suggesting a greater relative contribution to excursion. Each great toe muscle was found to have two intramuscular partitions arranged in a medial/lateral or superior/inferior orientation. The results of this study could be used to develop comprehensive *in vivo* ultrasound protocols to study the architecture of the medial and lateral great toe musculature in healthy subjects and those with HV.

### Conflict of Interest

No conflicts declared.

### Author Contributions

Project development: VC, MDV, TA, SAH, AA, DT; supervision: AA, DT; data collection: VC, MDV, TA, SAH; data analysis: VC, MDV; interpretation of the results: VC, MDV, TA, AA, DT; writing manuscript: VC, MDV, AA, DT; final check of the manuscript: VC, AA, DT.

### Ethics Approval

Ethics approval was received from the University of Toronto Health Sciences Research Ethics Board (Approval number: 27210).

### Funding

This study was funded by Carlton and Marguerite Smith Medical Research Fellowship award.

### Acknowledgements

The authors would like to acknowledge the donors who donated their bodies and tissue for research and education. Thank you to William Wood, Ian Bell, Trevor Robinson, and Sara Matias for their valuable technical assistance. The authors thank FARO Technologies for their generous technological support.

## References

1. Nix S, Smith M, Vicenzino B. Prevalence of hallux valgus in the general population: a systematic review and meta-analysis. J Foot Ankle Res 2010;3:21.
2. Dykyj D. Pathologic anatomy of hallux abducto valgus. Clin Podiatr Med Surg 1989;6:1–15.
3. Hoffmeyer P, Cox JN, Blanc Y, Meyer JM, Taillard W. Muscle in hallux valgus. Clin Orthop Relat Res 1988;(232):112–8.
4. Perera AM, Mason L, Stephens MM. The pathogenesis of hallux valgus. J Bone Joint Surg Am 2011;93:1650–61.
5. Incel NA, Genc H, Erdem HR, Yorgancioglu ZR. Muscle imbalance in hallux valgus: an electromyographic study. Am J Phys Med Rehabil 2003;82:345–9.
6. Iida M, Basmajian JV. Electromyography of hallux valgus. Clin Orthop Relat Res 1974;(101):220–4.
7. Mortka K, Lisi*f*ski P, Wiertel-Krawczuk A. The study of surface electromyography used for the assessment of abductor hallucis muscle activity in patients with hallux valgus. Physiother Theory Pract 2018;34:846–51.

8. Lieber RL, Ward SR. Skeletal muscle design to meet functional demands. Philos Trans R Soc Lond B Biol Sci 2011;366:1466–76.
9. Castanov V, Hassan SA, Shakeri S, Vienneau M, Zabjek K, Richardson D, McKee NH, Agur AMR. Muscle architecture of vastus medialis obliquus and longus and its functional implications: a three-dimensional investigation. Clin Anat 2019;32:515–23.
10. Li Z, Mogk JPM, Lee D, Bibliowicz J, Agur AM. Development of an architecturally comprehensive database of forearm flexors and extensors from a single cadaveric specimen. Comput Methods in Biomechanics and Biomedical Engineering: Imaging and Visualizaton 2015;3:3–12.
11. Shaw SM, Martino R, Mahdi A, Sawyer FK, Mathur S, Hope A, Agur AM. Architecture of the suprahyoid muscles: a volumetric musculoaponeurotic analysis. J Speech Lang Hear Res 2017;60:2808–18.
12. Kura H, Luo ZP, Kitaoka HB, An KN. Quantitative analysis of the intrinsic muscles of the foot. Anat Rec 1997;249:143–51.
13. Silver RL, de la Garza J, Rang M. The myth of muscle balance. A study of relative strengths and excursions of normal muscles about the foot and ankle. J Bone Joint Surg Br 1985;67:432–7.
14. Tosovic D, Ghebremedhin E, Glen C, Gorelick M, Mark Brown J. The architecture and contraction time of intrinsic foot muscles. J Electromyogr Kinesiol 2012;22:930–8.
15. Lachowitzer MR, Ranes A, Yamaguchi GT. Musculotendon parameters and musculoskeletal pathways within the human foot. J Appl Biomech 2007;23:20–41.
16. Ledoux WR, Hirsch BE, Church T, Caunin M. Pennation angles of the intrinsic muscles of the foot. J Biomech 2001;34:399–403.
17. Cralley JC, McGonagle W, Fitch K. The role of adductor hallucis in bunion deformity: part I. J Am Podiatry Assoc 1976;66:910–8.
18. Glasoe WM, Nuckley DJ, Ludewig PM. Hallux valgus and the first metatarsal arch segment: a theoretical biomechanical perspective. Phys Ther 2010;90:110–20.
19. Wong YS. Influence of the abductor hallucis muscle on the medial arch of the foot: a kinematic and anatomical cadaver study. Foot Ankle Int 2007;28:617–20.
20. Headlee DL, Leonard JL, Hart JM, Ingersoll CD, Hertel J. Fatigue of the plantar intrinsic foot muscles increases navicular drop. J Electromyogr Kinesiol 2008;18:420–5.
21. Farris DJ, Kelly LA, Cresswell AG, Lichtwark GA. The functional importance of human foot muscles for bipedal locomotion. Proc Natl Acad Sci U S A 2019;116:1645–50.
22. Kelly LA, Cresswell AG, Racinais S, Whiteley R, Lichtwark G. Intrinsic foot muscles have the capacity to control deformation of the longitudinal arch. J R Soc Interface 2014;11:20131188.
23. Kelikian AS. Sarrafian's anatomy of the foot and ankle: descriptive, topographic, functional. 3rd ed. Philadephia (PA): Wolters Kluwer Health; 2011. 736 p.
24. Martin BF. Observations on the muscles and tendons of the medial aspect of the sole of the foot. J Anat 1964;98:437–53.
25. Tas S, Cetin A. Mechanical properties and morphologic features of intrinsic foot muscles and plantar fascia in individuals with hallux valgus. Acta Orthop Traumatol Turc 2019;53:282–6.

**ORCID ID:**
V. Castanov 0000-0003-0918-6414; M. D. Vienneau 0000-0001-9799-2285; T. Arakawa 0000-0002-2653-9667; S. A. Hassan 0000-0001-8878-5567; A. Agur 0000-0002-2303-3628; D. Tyczynski 0000-0001-8134-0442

**Correspondence to:** Valera Castanov, PhD
Division of Anatomy, Department of Surgery, University of Toronto, Room 1158, Medical Sciences Building, 1 King's College Circle, Toronto, Ontario, Canada
Phone: (416) 978-8855
e-mail: vcastanov@qmed.ca.

*Conflict of interest statement:* No conflicts declared.

 *How to cite this article:* Castanov V, Vienneau MD, Arakawa T, Hassan SA, Agur A, Tyczynski D. Three-dimensional architecture of the great toe muscles: functional implications in hallux valgus. Anatomy 2020;14(2):77–85.